2014 Heliophysics School

DYNAMO LAB NOTES

Paul Charbonneau
Département de Physique
Université de Montréal

June 2014

Contents

Chapter 1

Kinematic axisymmetric dynamo models

It's not whether a thing is hard to understand.
It's whether, once understood, it makes any sense.

Hans Zinsser
Rats, Lice and History (1934)

These Notes contain information pertaining to the Laboratory component of the Lectures on stellar dynamos at the 2014 NASA Heliophysics Summer School. The Lab itelf consists in exploring the behavior of various types of dynamos as defining parameters are varied, as a means of interpreting observations of magnetic activity in late-type stars.

The truly impatients can skip directly to §1.5 and get going, but I strongly recommend that the preceeding sections be read at least rapidly, so as to know a bit how the dynamo solutions you will be working with are designed, and what the parameters you will be playing with relate to.

References to your *Heliophysics* textbooks are in the form Volume.chapter.section, e.g., III.6.2.1 refers to section 2.1 in chapter 6 of the third volume. I have also included a few homework problems and a short general bibliography at the end of the document.

1.1 Model design

The starting point is the magnetohydrodynamical induction equation (see §I.3.2):

$$\boxed{\frac{\partial \mathbf{B}}{\partial t} = \nabla \times (\mathbf{u} \times \mathbf{B} - \eta \nabla \times \mathbf{B})} \, . \tag{1.1}$$

where $\mathbf{u}$ is the total flow and η [$\mathrm{m}^2\,\mathrm{s}^{-1}$] the magnetic diffusivity. In the SI system of units, the the magnetic field $\mathbf{B}$ is measured in tesla (T).

We restrict ourselves here to kinematic, axisymmetric (two-dimensional) mean-field-like models, in the sense that we will be setting and solving partial differential equations for poloidal and toroidal large-scale magnetic components in a meridional $[r, \theta]$ plane, and subsume the effects of small-scale fluid motions and magnetic fields into coefficients of these PDEs (see §III.6.1). Working in spherical polar coordinates (r, θ, ϕ), the (time-indendent) large-scale flow and (time-dependent) magnetic field are expressed as

$$\mathbf{u}(r, \theta) = \mathbf{u}_p(r, \theta) + \varpi \Omega(r, \theta) \hat{\mathbf{e}}_\phi \ , \tag{1.2}$$

$$\mathbf{B}(r, \theta, t) = \nabla \times (A(r, \theta, t) \hat{\mathbf{e}}_\phi) + B(r, \theta, t) \hat{\mathbf{e}}_\phi \ . \tag{1.3}$$

where B is the large-scale toroidal (zonally-oriented) component of the magnetic field, the toroidal vector potential A defines the poloidal field, Ω [rad s^{-1}], is the rotational angular velocity, and $\mathbf{u}_p$ is a large-scale flow component contained in meridional planes $[r, \theta]$, like the poloidal magnetic field. Upon substituting these expressions into eq. (1.1), the latter can be separated into two coupled partial differential equations for A and B (see §III.6.1 ...and problem 1!):

$$\frac{\partial A}{\partial t} = \underbrace{\eta \left(\nabla^2 - \frac{1}{\varpi^2} \right) A}_{\text{resistive decay}} - \underbrace{\frac{\mathbf{u}_p}{\varpi} \cdot \nabla(\varpi A)}_{\text{advection}} + \underbrace{S(B)}_{\text{poloidal source}} , \tag{1.4}$$

$$\frac{\partial B}{\partial t} = \underbrace{\eta \left(\nabla^2 - \frac{1}{\varpi^2} \right) B}_{\text{resistive decay}} + \underbrace{\frac{1}{\varpi} \frac{\partial(\varpi B)}{\partial r} \frac{\partial \eta}{\partial r}}_{\text{diamagnetic transport}} - \underbrace{\varpi \nabla \cdot \left(\frac{B}{\varpi} \mathbf{u}_p \right)}_{\text{advection}} + \underbrace{\varpi (\nabla \times (A \hat{\mathbf{e}}_\phi)) \cdot \nabla \Omega}_{\text{shearing}} . \tag{1.5}$$

with $\varpi = r \sin\theta$ and we have already anticipated that the total magnetic diffusivity η will depend only on depth. The source term $S(B)$ in eq. (1.4), usually taken to depend on the toroidal field B, does *not* arise from the substitution of eqs. (1.2)–(1.3) into (1.1). Its *ad hoc* introduction in eq. (1.4) is however essential for sustained dynamo action, in order to bypass Cowling's theorem (see §I.3.3.8). Specific prescriptions for this source term are discussed further below in §1.2.5.

Numerical solutions to eqs. (1.4)—(1.5) are sought in a meridional $[r, \theta]$ quadrant, spanning

$$0.5 \leq r/R \leq 1 , \qquad 0 \leq \theta \leq \pi/2 , \tag{1.6}$$

where R is the star's radius. For solar-like dynamos, most of the action takes place in the convecting layers ($0.7 \leq r/R \leq 1$ for the sun), but the solution domain includes part of the underlying stably-stratified radiative core, as the latter can play a significant role in the storage and amplification of magnetic fields.

In the "exterior" $r > R$ there is only vacuum. Whatever solution we compute in $r < R$ must be matched to a current-free solution in $r > R$. For an axisymmetric magnetic field this translates into

$$\left(\nabla^2 - \frac{1}{\varpi^2} \right) A(r, \theta, t) = 0 , \tag{1.7}$$

$$B(r, \theta, t) = 0 . \tag{1.8}$$

Note in particular that the vector potential A must be continuous up to its first derivative normal to the surface, so that the magnetic field component tangential to the surface remains continuous across $r = R$. Regularity of the magnetic field on the symmetry axis ($\theta = 0$) requires that we set $B = 0$ there. Without any loss of generality, we can also set $A = 0$ on the axis.

The boundary condition imposed on the equatorial plane ($\theta = \pi/2$) sets the equatorial symmetry (parity) of the solutions. All dynamo solutions in the database have dipole-like (antisymmetric) polarity enforced by setting:.

$$\frac{\partial A(r, \pi/2)}{\partial \theta} = 0, \qquad B(r, \pi/2) = 0 , \qquad \text{[Antisymmetric]} , \tag{1.9}$$

while for symmetric (quadrupole-like) modes one would have set instead

$$A(r, \pi/2) = 0, \qquad \frac{\partial B(r, \pi/2)}{\partial \theta} = 0 , \qquad \text{[Symmetric]} . \tag{1.10}$$

1.2 Model ingredients

The numerical solution of eqs. (1.4)–(1.5) requires the specification of various functionals defining the inductive flows as well as source and dissipative terms. These are described in this section. In all cases we opt to use simple analytical parameterizations, either calibrated on observations, extracted from numerical simulations, and/or motivated on physical ground. For the illustrative purposes of this dynamo lab, this is entirely appropriate. Some of these models ingredients —or close variants thereof— are also discused in §III.6.2 of your *Heliophysics* textbooks.

1.2.1 The differential rotation

This is Ω in eq. (1.5). Differential rotation is driven by Reynolds stresses associated with turbulent convection and is essentially unavoidable in a rotating, convecting system (see §III.5.5). For $\Omega(r,\theta)$ we use here a simple solar-like parametrization, scaled in terms of the surface equatorial rotation rate:

$$\Omega(r,\theta) = \Omega_C + \frac{\Omega_S(\theta) - \Omega_C}{2}\left[1 + \mathrm{erf}\left(\frac{r - r_c}{w}\right)\right] , \tag{1.11}$$

where

$$\Omega_S(\theta) = (1 - a_2\cos^2\theta - a_4\cos^4\theta) \tag{1.12}$$

with parameter values $\Omega_C = 0.939$, $a_2 = 0.1264$, $a_4 = 0.1591$, $r_c/R = 0.7$, and $w/R = 0.05$, as inferred helioseismologically (see, e.g., Kosovichev 1996, ApJL, **469**, L61; Antia et al. 1998, MNRAS, **298**, 543; Charbonneau et al. 1999, ApJ, **527**, 445). Figure 1.1 below shows the corresponding isocontours of angular velocity, together with radial cuts at the pole, equator and mid-latitudes.

It should be noted that such a solar-like differential rotation profile is quite complex from the point of view of dynamo modelling, in that it is characterized by *three* partially overlapping shear regions: a strong positive radial shear in the equatorial regions of the tachocline, an even stronger negative radial shear in its polar regions, and a significant latitudinal shear throughout the convective envelope and extending partway into the tachocline. As shown on panel B of Fig. 1.1, for a tachocline of half-thickness $w/R = 0.05$, the mid-latitude latitudinal shear at $r/R = 0.7$ is comparable in magnitude to the equatorial radial shear; its potential contribution to dynamo action should not be casually dismissed. Conspicuously missing is the so-called surface shear layer also evidenced by helioseismology; it is usually deemed of secondary importance for internal dynamo action (but do see Brandenburg 2005, ApJ, **625**, 539).

1.2.2 The total magnetic diffusivity

This is η in eqs. (1.4)–(1.5). Assuming that the total magnetic diffusivity $\eta(r)$ varies only with depth, we use the same error-function radial profile as before, normalized to the turbulent diffusivity η_0 in the convective envelope:

$$\frac{\eta(r)}{\eta_0} = \Delta\eta + \frac{1 - \Delta\eta}{2}\left[1 + \mathrm{erf}\left(\frac{r - r_c}{w}\right)\right] . \tag{1.13}$$

The corresponding profile is plotted on Fig. 1.1 as a dash-dotted line. In practice, the core-to-envelope diffusivity ratio $\Delta\eta \equiv \eta_c/\eta_0$ is treated as a model parameter, with of course $\Delta\eta \ll 1$, since we associate η_c with the microscopic magnetic diffusivity, and η_0 with the presumably much larger mean-field turbulent diffusivity β (see §I.3.4.3). With the microscopic diffusivity $\eta_c \sim 1\,\mathrm{m^2 s^{-1}}$ below the core-envelope interface, and taking mean-field estimates of β at face value, one obtains $\Delta\eta \sim 10^{-9}$—10^{-6}. The solutions in the database you will be using have $\Delta\eta = 10^{-3}$—10^{-1}, which is much larger, but still small enough to nicely illustrate some important consequence of radial gradients in magnetic diffusivity.

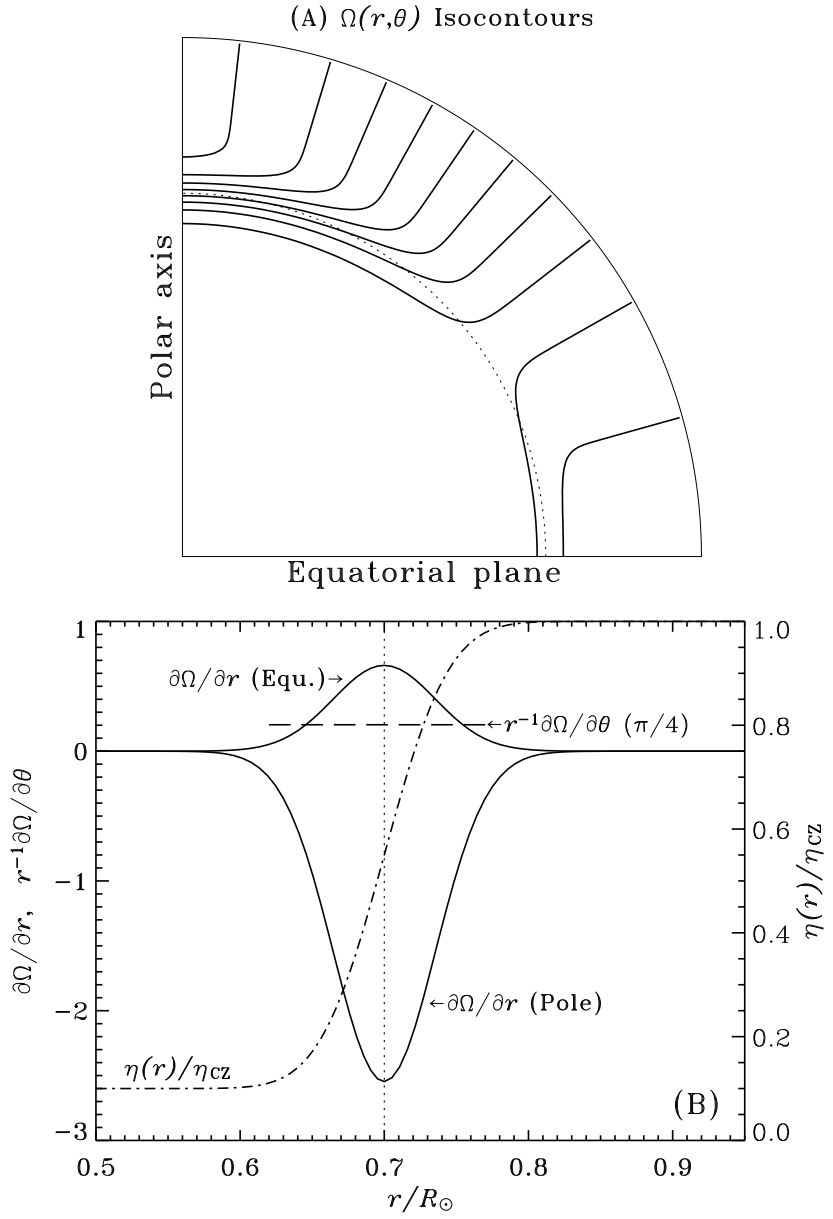

Figure 1.1: Isocontours of angular velocity generated by eqs. (1.11)—(1.12), with parameter values $w/R = 0.05$, $\Omega_C = 0.8752$, $a_2 = 0.1264$, $a_4 = 0.1591$ (panel A). The radial shear changes sign at colatitude $\theta = 55°$. Panel B shows the corresponding angular velocity gradients, together with the total magnetic diffusivity profile defined by eq. (1.13) (dash-dotted line, here with $\Delta\eta = 0.1$ for illustrative purposes). The core-envelope interface is located at $r/R = 0.7$ (dotted lines).

1.2.3 The meridional circulation

This is a contribution to $\mathbf{u}_p$ in eqs. (1.4)–(1.5), and denoted by $\mathbf{u}_\mathrm{M}$ in what follows. Meridional circulation is also unavoidable in turbulent rotating convective shells and results from an imbalance between Reynolds stresses and buoyancy forces (see §III.5.5). A $\sim 15\,\mathrm{m\ s^{-1}}$ poleward flow observed at the surface requires an equatorward return flow to satisfy mass conservation. Recent helioseismic measurements and analyses based on magnetic feature tracking suggest that this return flow occurs well within the convection zone, with multiple flow cells present in the convection zone (see Hathaway 2012, ApJ, **760**:id84; Zhao et al. 2013, ApJ, **774**, L29), although most dynamo models to date have used a monolithic single-cell per meridional quadrant.

For all models discussed below including a meridional circulation $\mathbf{u}_\mathrm{M}(r,\theta)$, we use the convenient parametric form, designed by van Ballegooijen & Choudhuri (1988, ApJ, **333**, 965). Their formulation allows the generation of a wide class of meridional flows, all satisfying the mass conservation ($\nabla\cdot(\rho\mathbf{u}_p)=0$) for a sun/star-like polytropic density profile.

For all dynamo solutions models considered here the model's parameters are set to define a steady quadrupolar circulation pattern, with a single flow cell per quadrant extending from the surface down to a depth r_b. Circulation streamlines are shown on Fig. 1.2, together with radial cuts of the latitudinal component at mid-latitudes ($\theta=\pi/4$), here for $r_b/R=0.675$. The flow is poleward in the outer convection zone, peaking at a speed u_0 at 45° latitude at the surface, with an equatorward return flow peaking slightly above the core-envelope interface, and rapidly vanishing below.

In the dynamo solution database, the only parameters that are varied are the mid-latitude surface flow speed u_0, and the lower extent r_b of the equatorward return flow.

1.2.4 Turbulent pumping

This is another contribution to $\mathbf{u}_p$ in eqs. (1.4)–(1.5), denoted by $\boldsymbol{\gamma}$ in what follows. Turbulent pumping is a pseudo-flow, in the sense that it is an advective contribution to the turbulent electromotive force in mean-field theory and so affects only the large-scale magnetic field (§I.3.4.3); a drop of ink dropped in the sun would not feel turbulent pumping!

The parameterization used here is inspired by measurements of turbulent pumping in MHD numerical simulations of solar convection (see, e.g., Käpylä et al. 2006, A&A, **455**, 401; Racine et al. 2011, ApJ, **735**:46). These measurements indicate that turbulent pumping is predominantly downwards in the bulk of the convection zone, with an equatorward latitudinal component peaking at low latitudes. Here we model this through:

$$\gamma_r(r) = -\gamma_0 f(r)\ , \tag{1.14}$$

$$\gamma_\theta(r,\theta) = \gamma_0 f(r)\sin^2\theta\cos\theta \tag{1.15}$$

where

$$f(r) = \frac{1}{4}\left[1+\mathrm{erf}\left(\frac{r-r_c}{d_1}\right)\right]\left[1-\mathrm{erf}\left(\frac{r-r_2}{d_2}\right)\right]\ . \tag{1.16}$$

with $d_1=0.025$, $r_2=0.85$, and $d_2=0.05$. The resulting radial profile $f(r)$ is plotted on Fig. 1.3. The quantity γ_0 [$\mathrm{m\ s^{-1}}$] measures the strength of turbulent pumping; this is the only parameter that is varied in the solution database, so that the ratio γ_r/γ_θ remains the same as γ_0 changes.

1.2.5 Poloidal source terms

This is S in eq. (1.4). Dynamo solutions for two classes of source terms are used in the solution database. The first is the classical local α-effect of mean-field electrodynamics (§I.3.4):

$$S(r,\theta,B(t)) = \alpha(r,\theta)B(r,\theta,t)\ , \qquad [\alpha\Omega] \tag{1.17}$$

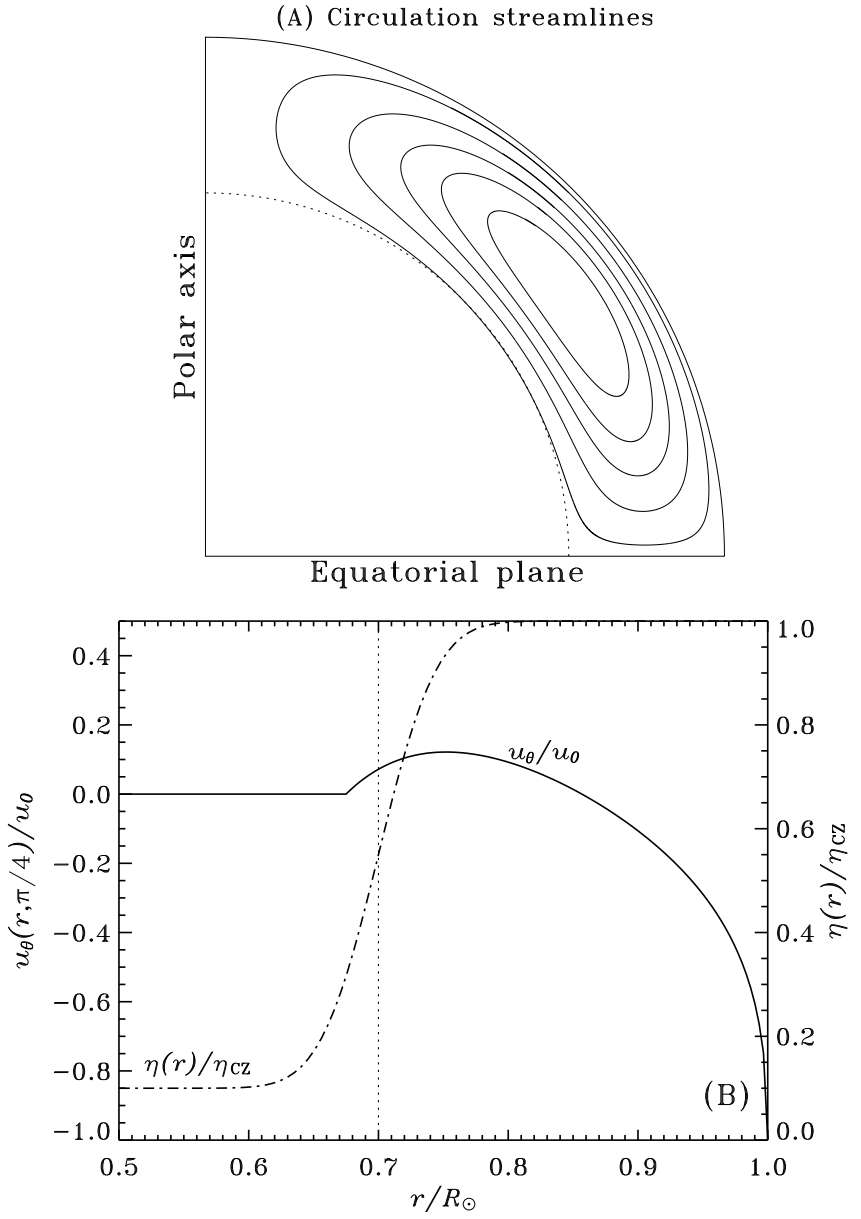

Figure 1.2: Streamlines of meridional circulation (panel A), together with the total magnetic diffusivity profile defined by eq. (1.13) (dash-dotted line, again with $\Delta\eta = 0.1$) and a mid-latitude radial cut of u_θ (bottom panel). The dotted line is the core-envelope interface r_c, and this specific realization of the van Ballegooijen & Choudhuri (1988) meridional flow has $m = 0.5$, $p = 0.25$, $q = 0$, and $r_b = 0.675$.

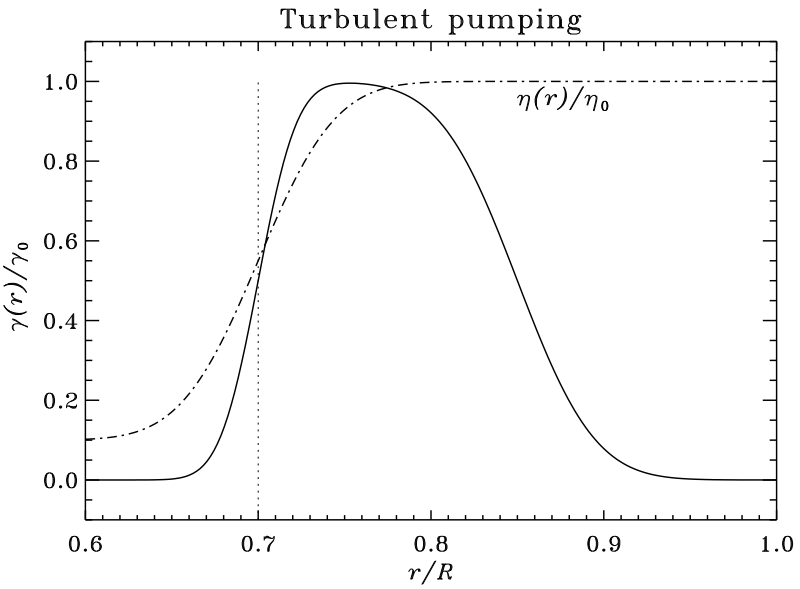

Figure 1.3: Radial profile of the turbulent pumping speed for all models in the solution database for which this physical effect is incorporated. Both the r- and θ-component of the turbulent pumping velocity share this profile, as defined by eq. (1.16) with parameter values $r_c = 0.7$, $d_1 = 0.025$, $r_2 = 0.85$, and $d_2 = 0.05$. The total magnetic diffusivity profile is shown as a dash-dotted line. The core-envelope interface is located at $r/R = 0.7$ (vertical dotted line).

where

$$\alpha(r,\theta) = \frac{s_0}{4}\left[1 + \mathrm{erf}\left(\frac{r-r_c}{d_1}\right)\right]\left[1 - \mathrm{erf}\left(\frac{r-r_2}{d_2}\right)\right]\cos(\theta)\ . \tag{1.18}$$

with parameter values $r_3 = 0.85$ and $d_2 = 0.05$, so that the radial dependency is the same as for the turbulent pumping speed $\boldsymbol{\gamma}$, reflecting the fact that the α-effect and turbulent pumping both arise from the same turbulent electromotive force (see §I.3.4.2). The combination of error functions concentrates the α-effect in the bottom half of the envelope, and let it vanish smoothly below, just as the net magnetic diffusivity does (i.e., we again set $r_c/R = 0.7$ and $d_1/R = 0.025$). The corresponding radial profile is plotted on Fig. 1.4. Various lines of argument point to an α-effect peaking in the bottom half the convective envelope, since there the convective turnover time is commensurate with the solar rotation period, a most favorable setup for the type of toroidal field twisting at the root of the α-effect. Likewise, the hemispheric dependence of the Coriolis force suggests that the α-effect should be positive in the Northern hemisphere, and change sign across the equator ($\theta = \pi/2$). The "minimal" latitudinal dependency is thus $\cos\theta$. These expectations are generally borne out by measurements of the α-tensor in MHD simulations of solar convection (e.g., Ossendrijver et al. 2001, A&A, **376**, 713; Käpylä et al. 2006, A&A, **455**, 401; Racine et al. 2011, ApJ, **735**:46; and references therein)

For dynamo models relying on the Babcock-Leighton mechanism of poloidal field regeneration, the source term S to be inserted in eq. (1.4) is given instead by:

$$S(r,\theta,B(t)) = s_0\, f(r)\sin\theta\cos\theta B(r_c,\theta,t)\ , \qquad [\mathrm{Babcock-Leighton}] \tag{1.19}$$

where

$$f(r) = \frac{1}{4}\left[1 + \mathrm{erf}\left(\frac{r-r_4}{d_4}\right)\right]\left[1 - \mathrm{erf}\left(\frac{r-r_5}{d_5}\right)\right]\ , \tag{1.20}$$

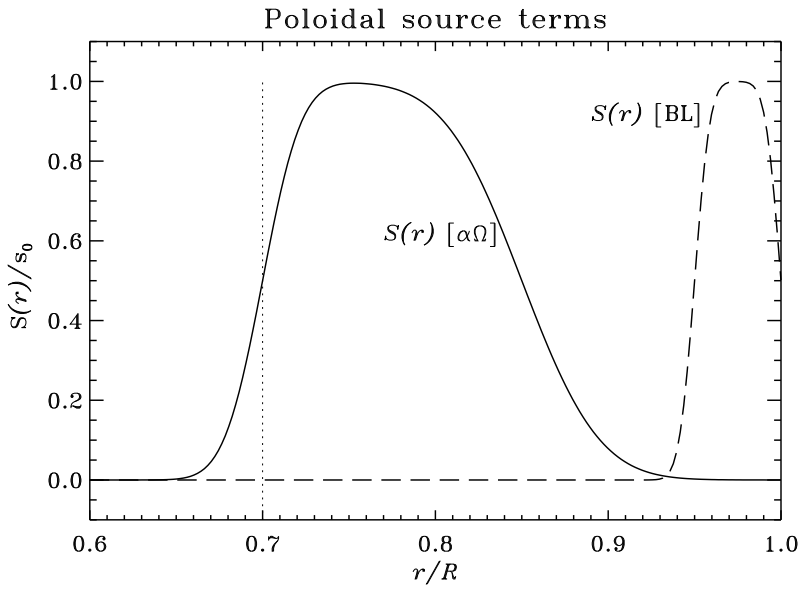

Figure 1.4: Radial profiles of the poloidal source terms for the $\alpha\Omega$ mean-field model (solid line), as defined by by eqs. (1.17)—(1.18), with parameter values $r_c = 0.7$, $d_1 = 0.025$, $r_3 = 0.85$, and $d_3 = 0.05$. The dashed line shows the radial profile for the Babcock-Leighton source term, as defined by by eqs. (1.19)—(1.20), with parameter values $r_4 = 0.95$, $d_4 = 0.01$, $r_5 = 1.0$, and $d_5 = 0.01$. The core-envelope interface is located at $r/R_\odot = 0.7$ (vertical dotted line).

where s_0 is a numerical coefficient setting the strength of the source term, and with the various remaining numerical coefficient taking the values $r_4 = 0.95$, $r_5 = 1$, $d_4 = d_5 = 0.01$. Note that the dependency on B is *non-local*, i.e., it involves the toroidal field evaluated at the core-envelope interface r_c, (but at the same polar angle θ). The combination of error functions concentrates the source term immediately beneath the surface, which is where the Babcock-Leighton mechanism is observed to operate. The $\sin\theta\cos\theta$ dependency is a first order description of Joy's Law, i.e., the tilt of active regions increases with latitude at low latitudes, but the tilts become randomized by convection for weakly magnetized flux ropes emerging at high latitudes. The nonlocality in B represents the fact that the strength of the source term is proportional to the field strength in the bipolar active region, itself presumably reflecting the strength of the diffuse toroidal field near the core-envelope interface, where the magnetic flux ropes eventually giving rise to the bipolar active region presumably originate.

This specific formulation of the Babcock-Leighton source term is taken directly from Dikpati & Charbonneau (1999, ApJ, **518**, 508), and has the practical advantage of being readily incorporated in the classical mean-field dynamo equations. A number of alternate but conceptually equivalent formulations do exist in the literature (e.g., Nandy & Choudhuri 2001, ApJ, **551**, 576; Munoz-Jaramillo et al. 2010, ApJ, **720**, L20; Yeates & Munoz-Jaramillo 2013, MNRAS, **436**, 3366).

Whether working with $\alpha\Omega$ or Babcock-Leighton models, all spatial dependencies are held fixed, with parameter values as specified above. The parameter s_0 measuring the overall magnitude of the poloidal source term is the only source-term-related parameter varying for all dynamo solutions in the database.

1.2.6 The amplitude-quenching nonlinearity

With the flow and source terms time-independent and specified a priori, eqs. (1.4)–(1.5) are linear in A and B and will accept eigensolutions $\propto \exp(st)$, with s a (complex) eigenvalue. For dynamo solutions, $\mathrm{Re}(s) > 0$ and unbounded exponential growth will ensue. To bypass this problem we introduce the simplest amplitude-limiting nonlinearity of common usage in solar/stellar dynamo modelling, namely the so-called "α-quenching". This consists in multiplying the source term amplitude parameter s_0 by a toroidal field-dependent prefactor which tends to zero as the field strength exceeds an equilibrium value $B_{\rm eq}$.

$$s_0 \rightarrow \frac{s_0}{1+(B(r,\theta,t)/B_{\rm eq})^2} \ , \tag{1.21}$$

where the equilibrium field strength $B_{\rm eq}$ then setting the absolute scale of the magnetic field amplitude. All solutions in the database use $B_{\rm eq} = 0.5\,\mathrm{T}$. Note that for the Babcock-Leighton source term, the toroidal field B on the RHS of this expression is evaluated at the core-envelope interface r_c rather than locally at r, in keeping ith the non-local nature of this poloidal source mechanism.

Notably missing in the Babcock-Leighton context is a lower toroidal field threshold on S, to mimic the fact that flux ropes with field strengths lower than a few teslas either fail to be destabilized in a short enough timescale, rise to the surface at high latitudes and without systematic tilt patterns, and/or fail altogether to survive their rise through the convective envelope. Including such a lower threshold has interesting consequences for the behavior of the resulting dynamo model (see, e.g., Charbonneau et al. 2005, ApJ, **619**, 613), but things being complicated enough as is, for this lab we'll just stick to the same algebraic amplitude-quenching nonlinearity for both classes of source terms.

Physically, the quenching nonlinearity intoduced in $\alpha\Omega$ models captures the fact that a stronger toroidal field is harder for cyclonic convection to twist and give rise to an α-effect (see §I.3.5.2 and III.6.2.1.2). In the Babcock-Leighton context, the nonlocal quenching nonlinearity reflects the fact that as the strength of the flux rope reaches about 2 T, it emerges without the East-West tilt essential to the Babcock-Leighton mechanism. (see §III.6.2.2).

1.3 Scalings, dynamo numbers and Reynolds numbers

With all "ingredients" specified, our next step is to put the dynamo equations into nondimensional form. This can actually be carried out in a number of ways. We opt here to scale all lengths in terms of the star's radius R, and time in terms of the corresponding diffusion time $\tau = R^2/\eta_0$. Equations (1.4)–(1.5) become

$$\frac{\partial A}{\partial t} = \left(\nabla^2 - \frac{1}{\varpi^2}\right) A - \frac{1}{\varpi}(\mathrm{R}_M \mathbf{u}_M + \mathrm{R}_T \boldsymbol{\gamma}) \cdot \nabla(\varpi A) + C_\alpha S \tag{1.22}$$

$$\frac{\partial B}{\partial t} = \left(\nabla^2 - \frac{1}{\varpi^2}\right) B \frac{1}{\varpi}\frac{\partial(\varpi B)}{\partial r}\frac{\partial \eta}{\partial r} - \varpi\nabla\cdot\left(\frac{B}{\varpi}(\mathrm{R}_M \mathbf{u}_M + \mathrm{R}_T \boldsymbol{\gamma})\right)$$

$$+ C_\Omega \varpi (\nabla \times A)\cdot(\nabla\Omega) \ , \tag{1.23}$$

where we have also explicitly separated the total poloidal flow $\mathbf{u}_p$ of eqs. (1.4)–(1.5) into its contributions arising from meridional circulation ($\mathbf{u}_M$, §1.2.3) and turbulent pumping ($\boldsymbol{\gamma}$, §1.2.4). The scaling procedure has led to the appearance of four nondimensional numbers:

$$C_\alpha = \frac{s_0 R}{\eta_0} \ , \tag{1.24}$$

$$C_\Omega = \frac{\Omega_0 R^2}{\eta_0} \ , \tag{1.25}$$

$$\mathrm{R}_M = \frac{u_0 R}{\eta_0} \ , \tag{1.26}$$

Meridal Flow Transport

$$\mathrm{R}_T = \frac{\gamma_0 R}{\eta_0} \ , \tag{1.27}$$

Turbulent pumping

with s_0 (dimension m s^{-1}), η_0 (dimension m^2 s^{-1}), u_0 (dimension m s^{-1}) γ_0 (dimension m s^{-1}) and Ω_0 (dimension rad s^{-1}) as reference values for the poloidal source, diffusivity, surface meridional flow, turbulent pumping speed, and shear, respectively. Remember that the functionals S, η, $\mathbf{u}_M$, $\boldsymbol{\gamma}$ and Ω are hereafter dimensionless quantities. The quantities C_α and C_Ω are **dynamo numbers**, measuring the importance of inductive versus diffusive effects on the RHS of eqs. (1.22)–(1.23). The other two dimensionless numbers, R_M and R_T, are Reynolds numbers, measuring the relative importance of advection (by meridional circulation for R_M, and by turbulent pumping for R_T) versus diffusion (by Ohmic dissipation) in the transport of A and B in meridional planes.

These four dimensionless parameters are the primary "knobs" with are varied when building dynamo models applicable to the sun and stars, so let's get some numerical estimates for their values. The turbulent diffusivity in the bulk of the solar convective envelope is estimated[1] to be

$$\eta_0 = 10^8 \, \mathrm{m}^2 \, \mathrm{s}^{-1} \ , \tag{1.28}$$

which yields a diffusion time:

$$\tau = \frac{R^2}{\eta_0} = 10^{10} \, \mathrm{s} \simeq 150 \, \mathrm{yr} \ . \tag{1.29}$$

For the sun,

$$\Omega_{\mathrm{eq}} = 2.6 \times 10^{-6} \, \mathrm{rad}^2 \, \mathrm{s}^{-1} \ , \tag{1.30}$$

so that

$$C_\Omega = 5 \times 10^4 \ , \tag{1.31}$$

With a surface meridional flow speed $u_0 \sim 15 \, \mathrm{m \ s}^{-1}$,

$$\mathrm{R}_M \simeq 100 \ , \tag{1.32}$$

while of the turbulent pumping speed extracted from numerical simulations suggest $\gamma_0 \sim 1 \, \mathrm{m \ s}^{-1}$, so that

$$\mathrm{R}_T \sim 10 \ . \tag{1.33}$$

Estimates for the source term amplitude of either the α-effect of $\alpha\Omega$ mean-field models, or of the Babcock-Leighton mechanism, are the most ill-constrained observationally. Values of a few m s^{-1} are often used, leading to C_α in the range 5–50.

[1] this being an extremely crude order-of-magnitude estimated based on the mixing length model of convection.

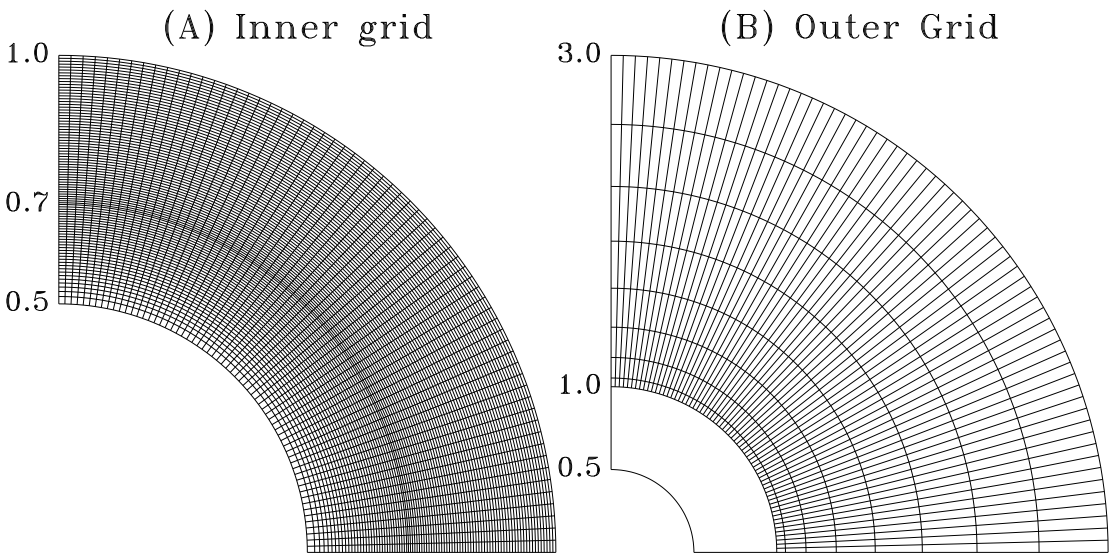

Figure 1.5: The computational grid in physical space. Part (A) shows the grid within the star's meridional quadrant, with the thick line indicating the core-envlope interface $r_c/R = 0.7$ for a "solar" model. Part (B) indicates the outer computational grid tiling the "buffer zone" within which the zero-current eqs. (1.7)–(1.8) are simultaneously solved. On each panel, the rotation (symmetry) axis runs vertically at left, and the equatorial plane horizontally at bottom. The grid shown here has dimension $N_r \times N_\theta = 96 \times 64$, which is used in all dynamo solutions included in the database. The computation itself is carried out on a cartesian grid in $[r/R, \cos\theta]$ space, with each cell tiled with a bilinear finite element.

1.4 Numerical implementation

Algorithmic details regarding how eqs. (1.22)–(1.23) are solved numerically matter little for this lab, but for those interested in such matters, what follows is a brief synopsis.

The solution domain is the N-hemisphere meridional plane, on which a 2D cartesian grid in $[r, \cos(\theta)]$ is defined. The dynamo equations are discretized on this grid using bilinear Galerkin finite elements. Although computationally heavier than finite differences, the use of finite elements has a number of practical advantages, most notably here the fact that the discretization error is not affected by the definition of a mesh where cells vary in size across the domain. This is important here because of the sharp gradients often building up in the vicinity of the core-envelope interface. The solutions included in the database are all computed on a (relatively) small grid of 96×64 in radius$\times$ latitude, as plotted on Figure 1.5.

Time stepping achieved through the implicit single-step Θ-method. Such an implicit scheme allows the use of relatively large time steps, making it possible to cover many cycles in a reasonably small number of time step, typically $\sim 10^3$. The overall code structure follows fairly closely that described in Burnett (1988, *Finite Element Analysis*, Reading:Addison-Wesley).

The initial condition is a weak global toroidal field, and the dynamo equations are integrated until the solutions has reached a statistically stationary state. At every time step, the poloidal vector potential and toroidal field values at every mesh node are written to file.

1.5 The solution database

The various tasks associated with the Lab (as detailed in §1.7 below) basically involve running $\alpha\Omega$ or Babcock-Leighton dynamo models, varying a subset of the defining parameters C_α, C_Ω, R_M, R_T, r_c, and/or r_b, and investigating the consequences of these variations on global

properties of the dynamo, with an eye towards interpreting the multiplicity of magnetic activity behavior observed in late-type stars. This being a HUGE undertaking, the first decision made was to focus on dynamo activity in main-sequence solar-type stars, i.e., stars with a radiative core overlaid by a convective envelope of significant thickness.

After much consideration, and in view of the limited time available to do this lab, it was decided to assemble a database of pre-calculated dynamo solutions, and let you mine that database as a means to explore the behavior of different classes of such models. Each solution file in the database has a name codified in such a manner as to ease the identification of the subset of solution files required to carry out the lab tasks defined in §1.7 below. Appendix A provides a list of all dynamo solutions included in the database, each identified by this filename. Here is an example of a file name:

$$\underbrace{\texttt{A0}}_{1}-\underbrace{\texttt{050}}_{2}-\underbrace{\texttt{010}}_{3}-\underbrace{\texttt{100}}_{4}-\underbrace{\texttt{000}}_{5}-\underbrace{\texttt{700}}_{6}-\underbrace{\texttt{675}}_{7} \tag{1.34}$$

The various 2- or 3-digit character or integer substrings of the filename correspond to the following, as numbered in the above:

1. A two-letter code indicating which type of dynamo this is; AO= a mean-field $\alpha\Omega$ dynamo, with a local poloidal source term given by eq. (1.17); BL= a Babcock-Leighton model, with a non-local surface source term given by eq. (1.19).

2. The value of the dimensionless dynamo number C_Ω, in units of 10^3; this is a measure of the strength of differential rotation.

3. The value of the dimensionless dynamo number C_α; this is a measure of the strength of the source term.

4. The value of the dimensionless Reynolds number R_M; this is effectively a measure of the surface poleward meridional flow speed.

5. The value of the dimensionless Reynolds number R_T; this is effectively a measure of the strength of turbulent pumping.

6. The radius r_c setting base of the convecting layers, in units of 10^{-3} of the star's radius
Different for different size stars 700 is typical for the Sun
7. The radius r_b setting the depth of the equatorward return meridional flow, in units of 10^{-3} of the star's radius.

Therefore, the file name given above contains a $\alpha\Omega$ dynamo solution computed with $C_\Omega = 5\times10^4$, $C_\alpha = 10$, $\mathrm{R}_M = 100$, $\mathrm{R}_T = 0$, with the base of the convection zone at $r/R = 0.7$ and the meridional return flow closing at $r/R = 0.675$.

The "`.i3e`" suffix flags this file as unformatted fortran-IEEE data. Don't try to view the file's content with a text editor, it will just look like junk. The IDL analysis routine provided to analyze the solutions (see below) is set up to properly read it. The advantages of storing the solutions as unformatted data are twofold: (1) smaller filesizes in the database, and (2) swifter read-in by the IDL analysis routine.

For each solution in the database, you will find a second file with the same name except for a "`.mpg`" suffix. This is a pre-computed animation of the solutions contained in each of the parent `.i3e` file, in mpeg format. Figure 1.6 details the format of these animations. Viewing these as you analyze the dynamo solutions will be a useful complement to the analyses carried out by the IDL analysis routine... to which we now turn.

1.6 The IDL analysis routine

Given that as a group you will be running the lab on a collection of laptop of varying speeds, ages, and operating systems, we opted to keep the bells and whistles to a minimum, and have you

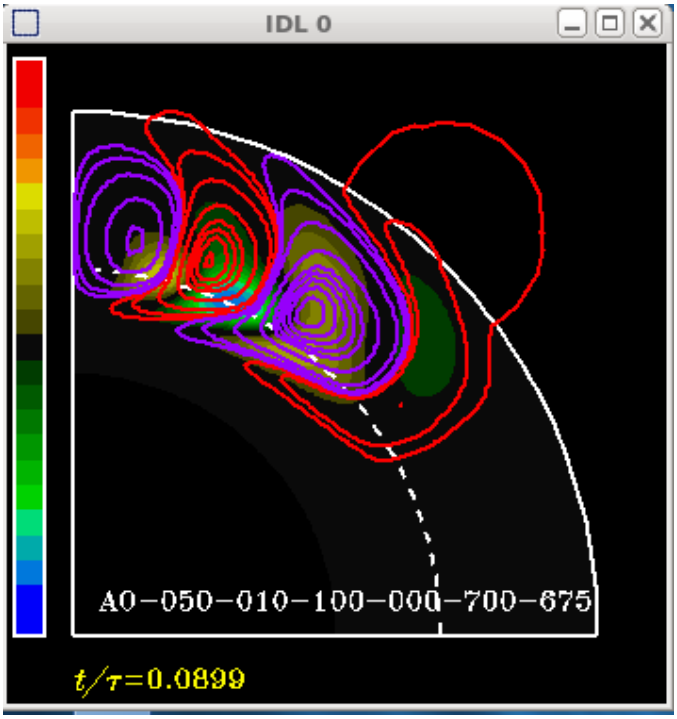

Figure 1.6: A representative single frame from the animations of a dynamo solution in the database. The animations show the toroidal magnetic field (color scale) with poloidal fieldlines superimposed, plotted in a meridional quadrant. The rotation axis runs vertically along the left, and the equatorial plane horizontally at bottom. Time is given in units of the diffusion time $\tau = R^2/\eta_0$, and the toroidal field is normalized to $[-1, 1]$, green-blue for negative values, yellow-red for positive.

do the lab using a single IDL routine which is fed a filename (following the naming convention explained in the preceding section), and carries out a series of postprocessing calculations and displays results in graphical form. Normally you should not have to touch/edit anything within this IDL files, but you will need to understand what graphical and numerical information is being produced.

1.6.1 Example IDL session

You will be given access to an IDL source file, named `helio14.idl`. The file contains a number of IDL procedures which must be compiled prior to running the main viewing procedure `viewdynamo`; this procedure requires three inputs:

1. A valid filename pointing to a file in the database, valid in the sense that it abides to the naming convection just explained.

2. A fractional radius at which the top time-latitude diagram of the toroidal field is constructed (see Fig. 1.7), the valid range being $[0.5, 1.0]$; if you enter a value outside of this range, a default value equal to the base of the convection zone r_c/R is used;

3. A latitude in degrees at which the middle time-radius diagram of the toroidal field is constructed (see Fig. 1.7), the valid range being $[0, 90]$; if you enter a value outside of this range, a default value of 45° is used.

Due to some unfortunate limitations inherent to the specific IDL implementation used at the Heliophysics School, these three parameters must be entered via an input file, which **must** be called `param.txt`, and contained three lines, e.g.:

```
A0-050-010-100-000-700-675.i3e
0.7
60.
```

Each line in this file corresponds to the following:

1. The filename from the database, following the naming convection just introduced. Here the file identified an $\alpha\Omega$ dynamo solution with parameter values $C_\alpha = 10$, $C_\Omega = 5 \times 10^4$, $\mathrm{R}_M = 100$, $\mathrm{R}_T = 0$, $r_c/R = 0.7$, and $r_b = 0.675$;
2. The second line identifies the depth, in fractional radius, at which the time-latitude diagram is to be constructed by the `viewdynamo` procedure. Here this is set at $r/R = 0.7$;
3. The third line identifies the latitude, in degrees, at which the time-latitude diagram is to be constructed by the `viewdynamo` procedure. Here this is set at 60°.

Detailed instructions on how to compile and run this analysis procedure will be given to you at the time of the Lab. As your first validation test, with the input file `param.txt` set as above, and if all goes well (!), the two windows reproduced on Figs. 1.7 and 1.8 should pop up on your screen. The information provided in these windows should allow you to carry out the task assigned to your group, as defined in §1.7 further below. Let's detail the content of each window in turn.

1.6.2 IDL Window 1

The top of IDL Window 1 first echoes the filename given as input. Immediately beneath follows a list (two leftmost columns) of input parameters to the dynamo solution, following the notation established in §1.2 of these Lab Notes. The third column lists (in yellow) useful physical (dimensional) quantities associated with the solution parameters, including the envelope magnetic diffusivity η_0, the diffusion time τ in years, the surface meridional flow speed and turbulent pumping speed, both in meters per second. The fourth column lists (in green) quantities extracted from the simulation output per se, namely (1) the peak toroidal field value at the core-envelope interface; (2) the peak surface radial field, both in Tesla; (3) the magnetic cycle period, in years.

The first graphical panel is a time-latitude diagram of the toroidal magnetic component $B(r, \theta, t)$ extracted the depth r/R specified in the `param.txt` input file. The equator is at bottom and the North-Pole on top, as indicated on the far left. This is usually considered the dynamo model's equivalent to the sunspot butterfly diagram. The color scale encodes the field strength, normalized to the peak value listed previously. The series of purple dots indicate the latitudes of peak toroidal field at each time step within this time-latitude slice. This, presumably, would correspond to the prefered latitude for sunspot emergences. On this and the two subsequent plots, only the second half of the dynamo run is plotted, to be better able to distinguish individual cycles, and time is in units of the diffusion time τ.

The middle graphical panel is now a time-radius slice extracted at the latitude specified in the `param.txt` input file, and normalized to the same peak field strength, as the preceding time-latitude diagram. The horizontal dashed line indicates the core-envelope interface r_c/R.

The bottom graphical panel is a time-latitude slice of the radial magnetic component at the surface ($r/R = 1$), normalized to the peak values given in the top-right column.

1.6.3 IDL Window 2

The second IDL window plots a time-series of the toroidal field extracted at point (r_c, θ_m) in the meridional plane, where r_c is the core-envelope interface and θ_m at which the radius-latitude

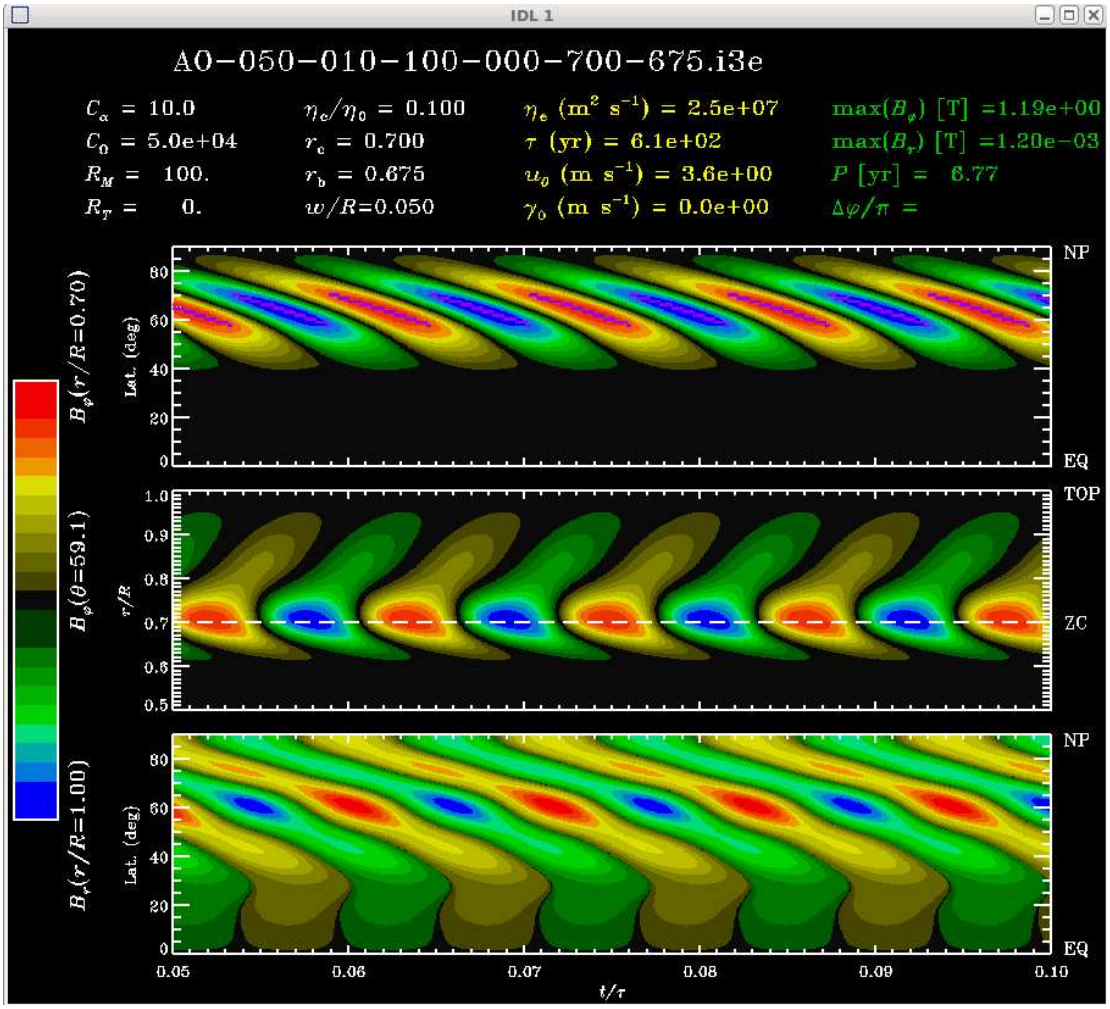

Figure 1.7: The first IDL window generated by the IDL procedure `viewdynamo`. Details in the text.

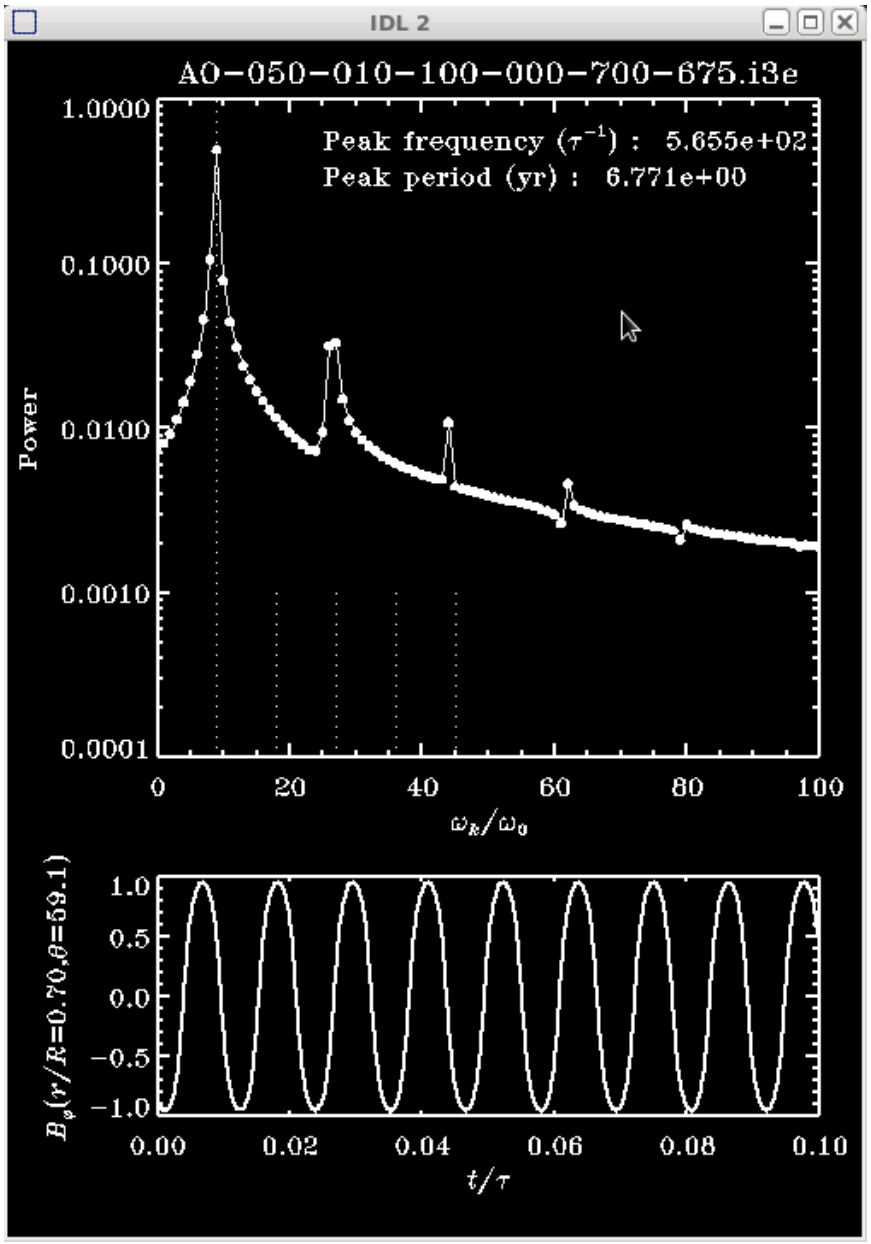

Figure 1.8: The second IDL window generated by the IDL procedure `viewdynamo`. Details in the text.

diagram in Window 1 is extracted. The top panels shows the power spectrum of this time series, computed by Fast Fourier Tranform. Note also that the vertical scale is logarithmic.

The vertical dotted line flags the peak frequency in the spectrum, listed at top right of the plot along with the cycle period The shorter dotted vertical line segments indicate the first 5 harmonics of the primary peak, which may or may not show significant power, according to the degree to which the underlying time series departs from sinusoidal shape.

1.7 The tasks

You are finally ready to get to work. The idea is that you will work in teams on one of the "tasks" detailed further below. This will involve working with either a $\alpha\Omega$ or Babcock-leighton dynamo model, and examine sequences of solutions from the database for which one or more defining parameters are varied. You will have to investigate how the properties of the dynamo solutions depend on the various physical mechanisms incorporated, albeit in simple form, in the dynamo model. You may want to produce your own plots of variations quantities (e.g., the cycle period) versus input parameters (e.g., the dynamo number C_α). Whether you choose to produce plots or not, each team should be ready to present a synopsis of their findings to the other teams at the end of the lab.

Here is a (non-exhaustive) list of quantities whose variations may be interesting to track as you work through your sequence of dynamo solutions:

1. The cycle period;
2. The ratio of surface poloidal to deep toroidal field; even though thre absolute scale of the magnetic field is set by our adopted algebraic α-quenching nonlinearity, this ratio remains a meaningful quantity.
3. The occurence of multiple dynamo modes, and/or long-timecale modulations of the dynamo solution. Both can arise through "interference" between dynamo modes feeding on distinct source regions, and do materialize in some corners of the parameter space for this dynamo model;
4. The concentration of the magnetic field at or beneath the core-envelope interface;
5. The concentration of the surface magnetic field at polar latitudes;

At the end of the Lab session, each team will report their findings to the whole group, as a starting point to our final discussion of stellar dynamos.

1.7.1 Impact of dynamo numbers on $\alpha\Omega$ dynamo solutions

The dynamo numbers C_α and C_Ω measure the strength of source terms in the $\alpha\Omega$ dynamo models. Increased rotation and luminosity may lead to increased differential rotation, and increased magnitude of α-effect, although theory and numerical simulations have not really been yielding consistent results, so all bets are still good. In this task you get to explore the dependency of a basic $\alpha\Omega$ dynamo on the strength of these two source terms, to get a feel for the impacts of changes in the rotation rate.

The idea is to begin with a "minimal" $\alpha\Omega$ dynamo model, and vary the dynamo numbers (parameters C_α and C_Ω). Here are a few specific queries and suggestions, to get you going:

1. Why is the dynamo mode confined to relatively high latitudes here, and why is the mode propagating equatorward ?
2. Examine how global quantities (period, peak toroidal field strength, poloidal/toroidal ratio, etc.) vary with C_α and C_Ω. Can you establish scaling relationships ?
3. Now look at how these quantities vary as a function of the *product* $C_\alpha \times C_\Omega$.

4. Do you see a change in the mode of dynamo action as you scan the $[C_\alpha, C_\Omega]$ plane ?

If lacking inspiration, see §III.6.2.1.1 and III.6.2.1.2 in your *Heliophysics* textbooks, as well as Saar & Brandenburg (1999, ApJ **524**, 295).

1.7.2 Impact of meridional flows in $\alpha\Omega$ dynamo solutions

Originally deemed unimportant in early dynamo models of the sun and stars, the meridional flow within convective envelope is now recognized as a potentially important dynamo ingredient. In particular, a deep equatorward return flow can drive a spatiotemporal evolution of the deep magnetic field in agreement with the sunspot butterfly diagram even if the signs of the α-effect and differential rotation run against the Parker-Yoshimura sign rule for equatorward progagation of the $\alpha\Omega$ dynamo wave. However, too strong a meridional flow can also impact the very operation of mean-field dynamos. You get to explore this in this task.

The idea is to begin with a "minimal" $\alpha\Omega$ dynamo model, and vary the meridional flow speed (through parameter R_M) and depth of return flow (parameter r_b). Here are a few specific queries and suggestions, to get you going:

1. Starting with the $\mathrm{R}_M = 0$ solution, why is the dynamo mode confined to relatively high latitudes here, and why is the mode propagating equatorward ?

2. What happens to the dynamo period as the meridional flow speed increases (via increasing R_M)?

3. Do you perceive a transition in the mode of dynamo action, as R_M is increased ? Is this transition abrupt or gradual ? How do you think it originates ?

4. Are your findings robust with respect to changes in the depth of the meridional equatorward return flow ?

If lacking inspiration, see §III.6.2.1.4 in your *Heliophysics* textbooks.

1.7.3 Impact of turbulent pumping in $\alpha\Omega$ dynamo solutions

Turbulent pumping is an avoidable part of the turbulent electromotive force in inhomogeneous turbulence lacking reflectional symmetry, which is the case in the rotating, stratified interiors of the sun and stars. Turbulent pumping acts to transport the large-scale magnetic field, usually downwards and equatorward according to recent numerical simulations, and so can impact the spatiotemporal distributions of the cyclic magnetic field. You get to explore this in this task.

The idea is to begin with a "minimal" $\alpha\Omega$ dynamo model with fixed $C_\alpha = 10$, and vary the turbulent pumping speed (through parameter R_T). Then verify whether the patterns you observe (or not...) are sensitively dependent on the dynamo number C_α, which is the other key piece of the turbulent electromotive force in such models. Here are a few specific queries and suggestions, to get you going:

1. Is the cycle morphology impacted by turbulent pumping ?

2. Is the cycle period impacted by turbulent pumping ?

3. Turbulent pumping is downward-directed in the bulk of the convection zone and vanishes by construction in its outer half; yet the surface magnetic field distribution is affected by the inclusion of turbulent pumping. Why ?

4. What happens if you increase both C_α and R_T by the same factors ?

If lacking inspiration, see Käpylä et al. (2006, Astr. Nach., **327**, 884).

1.7.4 Meridional flows in Babcock-Leighton dynamos – part I

Current state of the sun

In dynamo models of the Babcock-Leighton variety, the poloidal source term is concentrated close to the surface layers, while the shearing producing the toroidal field is localized deeper in the convection one; consequently, a transport mechanism is required to connect the two source regions and close the dynamo loop. The meridional flow (§1.2.3) is an obvious candidate, and you get to explore this in this task.

The idea is to examine a sequence of solutions with increasing R_M, and see to what degree your finding depend on the value of the dynamo numbers C_α and C_Ω. Here are a few specific queries and suggestions, to get you going:

1. Starting with the $\mathrm{R}_M = 0$ solution, you do get cyclic dynamo action; how do you think the two source regions are connected here ?
2. What happens to the dynamo period as the meridional flow speed increases (via increasing R_M)?
3. Do you perceive a transition in the mode of dynamo action, as R_M is increased ? Is this transition abrupt or gradual ?
4. If you change the values of the dynamo numbers, is the cycle period affected ? Why ?

If lacking inspiration, see Dikpati & Charbonneau (1999, ApJ, **518**, 508).

1.7.5 Meridional flows in Babcock-Leighton dynamos – part II

In dynamo models of the Babcock-Leighton variety, the meridional flow acts as a "conveyor belt" linking the two magnetic source regions, namely the surface layers, where the Babcock-Leighton mechanism of poloidal field generation is operating, and the base of the convection zone, where shearing by differential rotation induces the toroidal component. But what happens if this conveyor belt does not extend all the way to the base of the convection zone, as suggested by recent helioseismic inversions of the meridional flow ? You get to tackle this issue in this task.

The idea is to fix the meridional flow speed at a value $\mathrm{R}_M = 500$, and investigate the consequences of varying the depth of the return flow, via the parameter r_b. If time allows, see also to what degree your finding depend on the value of the dynamo numbers C_α and C_Ω. Here are a few specific queries and suggestions, to get you going:

1. If you change the depth of the equatorward return flow, is the cycle period affected ? Why ?
2. Do you perceive a transition in the mode of dynamo action, as r_b is varied ? Is this transition abrupt or gradual ?
3. If you change the values of the dynamo numbers, is the cycle period affected ? Why ?

If lacking inspiration, see Jouve & Brun (2007, A&A, **474**, 239).

1.7.6 Impact of turbulent pumping in Babcock-Leighton models with shallow meridional flows

Alternative Mode of Tranport

Recent helioseismic determinations of the meridional flow deep in the convection zone have revealed a multi-celled structure rather different from Fig. 1.2, which has led to various obituary notices for flux transport dynamos in general, and Babcock-Leighton models in particular. Yet what really matters is that the surface regions be "connected" to the deep convection zone, and mechanisms other than the meridional flow exist. You get to explore the impact of one such mechanism in this task.

The basic idea is to start with a few Babcock-Leighton dynamo solutions with the meridional flow confined to the outer envelope, and examine how the solution characteristics change as the turbulent pumping speeds are increased (via an increase in the R_T parameter). Then you check on the robustness of your conclusions by varying the Reynolds number R_M. Here are a few specific queries and suggestions, to get you going:

1. Is turbulent pumping leading to a change in the mode of dynamo action in this model ? Why ?
2. Can you do away altogether with the meridional flow, and still have a viable Babcock-Leighton model ?
3. How does the cycle period and dynamo mode of such a $\mathrm{R}_M = 0$ model depend on R_T ? Are any morphological transitions taking place ?

If lacking inspiration, see Guerrero & Gouveia Dal Pino (2008, A&A, **485**, 267), and/or Pipin & Kosovichev (2013, ApJ, **776**:id36).

Not Sun Like

1.7.7 Impact of deepening convection zone on $\alpha\Omega$ dynamo solutions

Running down the main-sequence, stars progressively less massive and luminous than the sun have a convection zone that gains in depth until a point where they are fully convective from center to surface. How this may translate into significant changes in the mode of dynamo action has been the subject of many speculations but very little systematic modelling work. This is what you get to explore in this task.

The idea is to pick a representative classical $\alpha\Omega$ dynamo solution, more specifically one with $C_\alpha = 10$, $C_\Omega = 5 \times 10^4$, $\mathrm{R}_M = 0$, and $\mathrm{R}_T = 0$, and simply investigate what happens to the dynamo mode as the parameter r_c is varied. Note that by varying r_c, you are changing the depth at which the magnetic diffusivity profile falls from high to low values (Fig. 1.1, dash-dotted line), the position of the tachocline shear layer, as well as the depth at which the α-effect falls to zero (Fig. 1.4). Whatever the value of r_c, the α-effect remains confined to the bottom half of the convection zone, i.e., $r_2 = r_c + (1 - r_c)/2$ in eq. (**??**). Here are a few specific queries and suggestions, to get you going:

1. Is the cycle period changing ? why ?
2. Is the spatial distribution of the dynamo mode simply "stretching vertically" with the change in r_c ?
3. Why is the ratio of radial to toroidal field changing significantly with r_c, even though the ratio C_α/C_Ω remains constant ?
4. Is the surface magnetic field much affected by changes in r_c ? why ?

Not Sun Like

1.7.8 Impact of deepening convection zone on Babcock-Leighton dynamo solutions

Running down the main-sequence stars, stars progressively less massive and luminous than the sun have a convection that gains in depth until a point where it is fully convective from center to surface. Much has been speculated in the possible "failure" of Babcock-Leighton dynamos once the tachocline gets displaced deeper and deeper in the interior, and eventually disappears in fully convective stars. This is what you get to explore in this task.

The idea is to pick a representative Babcock-Leighton dynamo solution, more specifically with $C_\alpha = 10$, $C_\Omega = 5 \times 10^4$, $\mathrm{R}_M = 500$, and $\mathrm{R}_T = 0$, and investigate what happens to the dynamo mode as the parameters r_c and r_b are varied, assuming $r_b = r_c$ in all cases, i.e., the equatorward meridional return flow extends to the base of the convective layers but not

deeper. Note that by varying r_c, you are also changing the depth at which the magnetic diffusivity profile falls from high to low values (Fig. 1.1, dash-dotted line), and the position of the tachocline shear layer. The Babcock-Leighton source term, on the other hand, remains confined to the upper 5% of the star in all cases (see Fig. 1.4, dashed line). Here are a few specific queries and suggestions, to get you going:

1. Is the cycle period changing ? why ?
2. Is the spatial distribution of the dynamo mode simply "stretching vertically" with the change in r_c ?
3. Is the surface magnetic field much affected by changes in r_c ? why ?

Problems:

1. Obtain equations (1.4) and (1.5) by substitution of eqs. (1.2) and (1.3) into the MHD induction equation (1.1). Hint: the induction equation is a vector equation; terms "oriented" in the ϕ-direction must cancel one another independently of terms oriented perpendicular to the ϕ-direction.
2. Let's consider a constant-density "sun" made of purely ionized Hydrogen. Suppose now that its *exterior magnetic* field can be approximated by a dipole, with a surface field strength of 10^{-3} T. Assume now that this magnetic field is produced by an azimuthal (i.e., ϕ-directed) current density within the interior ($r/R_\odot < 1$); then,
   (a) Estimate the magnitude of the current density required to produce such a dipolar field;
   (b) Estimate the drift velocity between protons and electrons required to produce such a current density. How does it compare to the average thermal velocity?
   (c) How can such a small velocity difference not be erased by collisions between microscopic constituents? To answer this one will have to think back to some fundamental aspects of the induction process, as covered in your first course on electromagnetism.
3. Consider the case of shearing of a pure dipole by the parametrized solar-like differential rotation of §1.2.1 herein;
   (a) Starting from a poloidal field strength of 10^{-4} T at the core-envelope interface, calculate/estimate the time taken for the toroidal field strength to reach a strength of 1 T;
   (b) In a differentially rotating axisymmetric and inviscid fluid sphere such as considered here, the ϕ-component of the momentum equation reduces to:

$$\rho\varpi\frac{\partial\Omega}{\partial t} = \frac{1}{\mu_0\varpi}\mathbf{B}_p\cdot\nabla(\varpi\, B_\phi)$$

   where $\mathbf{B}_p \equiv B_r\hat{\mathbf{e}}_r + B_\theta\hat{\mathbf{e}}_\theta$, $\varpi = r\sin\theta$, and $\mu_0 = 4\pi\times10^{-7}$ N A^{-2} is the magnetic permeability of vacuum. By judicious dimensional analysis of this expression, evaluate the timescale over which the rotational shear at the core-envelope interface would be altered by the Lorentz force, once the toroidal field strength has reached 1T;
   (c) Is your result in (b) much longer or shorter than the solar cycle period? What does this suggest?

Bibliography:

If you need a refresher on undergraduate electromagnetism, you should go back to

Griffith, D.J., *Introduction to Electrodynamics*, 3rd ed., Prentice Hall (1999).

At the graduate level, the standard reference remains

Jackson, J.D., *Classical Electrodynamics*, 2nd ed., John Wiley & Sons (1975),

who does devote a chapter to magnetohydrodynamics, including a discussion of magnetic wave modes. My personal favorite on magnetohydrodynamics is:

Davidson, P.A., *An Introduction to Magnetohydrodynamics*, Cambridge University Press (2001).

Further specializing to the dynamo problem, the all-time classic is:

Moffatt, H.K. 1978, *Magnetic Field Generation in Electrically Conducting Fluids*, (Cambridge: Cambridge Univ. Press).

For more on dynamo models for the sun (and, by extension, solar-type stars), see the following recent review paper and monograph authored by yours very truly:

Charbonneau, P., 2010, LRSP, **7**,
`http://solarphysics.livingreviews.org/Articles/lrsp-2010-3/`
Charbonneau, P., 2013, *Solar and stellar dynamos*, Saas-Fee Advanced Course 39 (2009), ed. O. Steiner, Berlin: Springer

Appendix A

The dynamo solution database

The following two Tables list all names and defining parameter values of the dynamo solutions included in the database. Animation files have the same name, except for a "`.mpg`" suffix instead of "`.i3e`". Table 1 lists the $\alpha\Omega$ dynamo solutions, and Table 2 the Babcock-Leighton flux transport solutions. The naming convention is explained in §1.5.

Table 1
The $\alpha\Omega$ dynamo solutions

File Name	Model type	C_α	C_Ω	R_M	R_T	r_c	r_b
AO-030-005-000-000-700-675.i3e	$\alpha\Omega$	5	3×10^4	0	0	0.7	0.675
AO-060-005-000-000-700-675.i3e	$\alpha\Omega$	5	6×10^4	0	0	0.7	0.675
AO-120-005-000-000-700-675.i3e	$\alpha\Omega$	5	1.2×10^5	0	0	0.7	0.675
AO-240-005-000-000-700-675.i3e	$\alpha\Omega$	5	2.4×10^5	0	0	0.7	0.675
AO-030-010-000-000-700-675.i3e	$\alpha\Omega$	10	3×10^4	0	0	0.7	0.675
AO-060-010-000-000-700-675.i3e	$\alpha\Omega$	10	6×10^4	0	0	0.7	0.675
AO-120-010-000-000-700-675.i3e	$\alpha\Omega$	10	1.2×10^5	0	0	0.7	0.675
AO-240-010-000-000-700-675.i3e	$\alpha\Omega$	10	2.4×10^5	0	0	0.7	0.675
AO-030-020-000-000-700-675.i3e	$\alpha\Omega$	20	3×10^4	0	0	0.7	0.675
AO-060-020-000-000-700-675.i3e	$\alpha\Omega$	20	6×10^4	0	0	0.7	0.675
AO-120-020-000-000-700-675.i3e	$\alpha\Omega$	20	1.2×10^5	0	0	0.7	0.675
AO-240-020-000-000-700-675.i3e	$\alpha\Omega$	20	2.4×10^5	0	0	0.7	0.675
AO-050-010-030-000-700-675.i3e	$\alpha\Omega$	10	5×10^4	30	0	0.7	0.675
AO-050-010-050-000-700-675.i3e	$\alpha\Omega$	10	5×10^4	50	0	0.7	0.675
AO-050-010-100-000-700-675.i3e	$\alpha\Omega$	10	5×10^4	100	0	0.7	0.675
AO-050-010-200-000-700-675.i3e	$\alpha\Omega$	10	5×10^4	200	0	0.7	0.675
AO-050-010-300-000-700-675.i3e	$\alpha\Omega$	10	5×10^4	300	0	0.7	0.675
AO-050-010-500-000-700-675.i3e	$\alpha\Omega$	10	5×10^4	500	0	0.7	0.675
AO-050-010-800-000-700-675.i3e	$\alpha\Omega$	10	5×10^4	800	0	0.7	0.675
AO-050-010-300-000-700-650.i3e	$\alpha\Omega$	10	5×10^4	300	0	0.7	0.65
AO-050-010-300-000-700-700.i3e	$\alpha\Omega$	10	5×10^4	300	0	0.7	0.7
AO-050-010-300-000-700-725.i3e	$\alpha\Omega$	10	5×10^4	300	0	0.7	0.725
AO-050-010-300-000-700-750.i3e	$\alpha\Omega$	10	5×10^4	300	0	0.7	0.75
AO-050-010-000-002-700-700.i3e	$\alpha\Omega$	10	5×10^4	0	2	0.7	0.7
AO-050-010-000-005-700-700.i3e	$\alpha\Omega$	10	5×10^4	0	5	0.7	0.7
AO-050-010-000-010-700-700.i3e	$\alpha\Omega$	10	5×10^4	0	10	0.7	0.7
AO-050-010-000-020-700-700.i3e	$\alpha\Omega$	10	5×10^4	0	20	0.7	0.7
AO-050-010-000-030-700-700.i3e	$\alpha\Omega$	10	5×10^4	0	30	0.7	0.7
AO-050-010-000-050-700-700.i3e	$\alpha\Omega$	10	5×10^4	0	50	0.7	0.7
AO-050-020-000-020-700-700.i3e	$\alpha\Omega$	20	5×10^4	0	20	0.7	0.7
AO-050-050-000-050-700-700.i3e	$\alpha\Omega$	50	5×10^4	0	50	0.7	0.7
AO-050-010-000-000-600-600.i3e	$\alpha\Omega$	10	5×10^4	0	0	0.6	0.6
AO-050-010-000-000-650-650.i3e	$\alpha\Omega$	10	5×10^4	0	0	0.65	0.65
AO-050-010-000-000-700-700.i3e	$\alpha\Omega$	10	5×10^4	0	0	0.7	0.7
AO-050-010-000-000-750-750.i3e	$\alpha\Omega$	10	5×10^4	0	0	0.75	0.75
AO-050-010-000-000-800-800.i3e	$\alpha\Omega$	10	5×10^4	0	0	0.8	0.8
AO-050-010-000-000-850-850.i3e	$\alpha\Omega$	10	5×10^4	0	0	0.85	0.85
AO-050-010-000-000-900-900.i3e	$\alpha\Omega$	10	5×10^4	0	0	0.9	0.9

Table 2
The Babcock-Leighton dynamo solutions

File Name	Model type	C_α	C_Ω	R_M	R_T	r_c	r_b
BL-050-010-000-000-700-675.i3e	B-L	10	5×10^4	0	0	0.7	0.675
BL-050-010-010-000-700-675.i3e	B-L	10	5×10^4	10	0	0.7	0.675
BL-050-010-100-000-700-675.i3e	B-L	10	5×10^4	100	0	0.7	0.675
BL-050-010-200-000-700-675.i3e	B-L	10	5×10^4	200	0	0.7	0.675
BL-050-010-300-000-700-675.i3e	B-L	10	5×10^4	300	0	0.7	0.675
BL-050-010-500-000-700-675.i3e	B-L	10	5×10^4	500	0	0.7	0.675
BL-050-010-800-000-700-675.i3e	B-L	10	5×10^4	800	0	0.7	0.675
BL-050-010-500-000-700-600.i3e	B-L	10	5×10^4	500	0	0.7	0.6
BL-050-010-500-000-700-650.i3e	B-L	10	5×10^4	500	0	0.7	0.65
BL-050-010-500-000-700-700.i3e	B-L	10	5×10^4	500	0	0.7	0.7
BL-050-010-500-000-700-725.i3e	B-L	10	5×10^4	500	0	0.7	0.725
BL-050-010-500-000-700-750.i3e	B-L	10	5×10^4	500	0	0.7	0.75
BL-050-010-500-000-700-800.i3e	B-L	10	5×10^4	500	0	0.7	0.8
BL-050-010-500-000-700-900.i3e	B-L	10	5×10^4	500	0	0.7	0.9
BL-100-005-500-000-700-700.i3e	B-L	5	10^5	500	0	0.7	0.7
BL-100-010-500-000-700-800.i3e	B-L	10	10^5	500	0	0.7	0.8
BL-050-020-500-000-700-900.i3e	B-L	20	5×10^4	500	0	0.7	0.9
BL-050-010-500-000-700-850.i3e	B-L	10	5×10^4	500	0	0.7	0.85
BL-050-010-500-005-700-850.i3e	B-L	10	5×10^4	500	5	0.7	0.85
BL-050-010-500-010-700-850.i3e	B-L	10	5×10^4	500	10	0.7	0.85
BL-050-010-500-020-700-850.i3e	B-L	10	5×10^4	500	20	0.7	0.85
BL-050-010-500-030-700-850.i3e	B-L	10	5×10^4	500	30	0.7	0.85
BL-050-010-500-040-700-850.i3e	B-L	10	5×10^4	500	40	0.7	0.85
BL-050-010-500-050-700-850.i3e	B-L	10	5×10^4	500	50	0.7	0.85
BL-050-010-100-020-700-850.i3e	B-L	10	5×10^4	100	20	0.7	0.85
BL-050-010-200-020-700-850.i3e	B-L	10	5×10^4	200	20	0.7	0.85
BL-050-010-800-020-700-850.i3e	B-L	10	5×10^4	800	20	0.7	0.85
BL-050-010-500-020-700-850.i3e	B-L	10	5×10^4	500	20	0.7	0.85
BL-050-010-000-005-700-850.i3e	B-L	10	5×10^4	000	5	0.7	0.85
BL-050-010-000-010-700-850.i3e	B-L	10	5×10^4	000	10	0.7	0.85
BL-050-010-000-020-700-850.i3e	B-L	10	5×10^4	000	20	0.7	0.85
BL-050-010-500-000-600-600.i3e	B-L	10	5×10^4	500	0	0.6	0.6
BL-050-010-500-000-650-650.i3e	B-L	10	5×10^4	500	0	0.65	0.65
BL-050-010-500-000-700-700.i3e	B-L	10	5×10^4	500	0	0.7	0.7
BL-050-010-500-000-750-750.i3e	B-L	10	5×10^4	500	0	0.75	0.75
BL-050-010-500-000-800-800.i3e	B-L	10	5×10^4	500	0	0.8	0.8
BL-050-010-500-000-850-850.i3e	B-L	10	5×10^4	500	0	0.85	0.85